

# Resonant infrared laser-induced desorption of CD<sub>3</sub>F condensed on NaCl(100)

Britta Redlich,<sup>\*a</sup> Helmut Zacharias,<sup>b</sup> Gerard Meijer<sup>ac</sup> and Gert von Helden<sup>a</sup>

<sup>a</sup> FOM Institute for Plasma Physics Rijnhuizen, P.O. Box 1207, 3430 BE, Nieuwegein, The Netherlands. E-mail: brittar@rijnh.nl; Fax: +31 30-6031204; Tel: +31 30-6096999

<sup>b</sup> Westfälische Wilhelms-Universität Münster, Wilhelm-Klemm-Str. 10, 48149, Münster, Germany

<sup>c</sup> Department of Molecular and Laser Physics, University of Nijmegen, Toernooiveld 1, 6525 ED, Nijmegen, The Netherlands

Received 22nd February 2002, Accepted 24th April 2002

First published as an Advance Article on the web 11th June 2002

In investigations of the dynamics of the desorption of molecules from surfaces, a selective excitation of specific molecular vibrations is desirable. We here report studies on the infrared laser-induced desorption of CD<sub>3</sub>F condensed on the NaCl(100) single crystal surface, in which the intramolecular vibrations of the CD<sub>3</sub>F molecules are directly excited. Desorption of the intact molecules is monitored using electron impact ionization followed by mass-selective detection in a quadrupole mass spectrometer. Desorption only occurs when the excitation laser is at 9.0, 10.5, 9.4, or 11.0 μm, corresponding to excitation on the  $\nu_2$ ,  $\nu_3$ ,  $\nu_5$ , and  $\nu_6$  modes of CD<sub>3</sub>F. An analysis of the time-of-flight spectra as a function of the laser fluence is presented. Different desorption mechanisms are discussed.

## Introduction

Desorption of molecules from surfaces constitutes one of the fundamental processes of heterogeneous surface reactions. One of the major goals is to understand the energy flow in these adsorbate systems to gain a detailed understanding of the underlying processes.

It is well known that the excitation of electronic transitions using (ultrafast) UV or VIS laser pulses in a layer adsorbed on a metal substrate can lead to desorption, see *e.g.* ref. 1 and references therein. In those experiments, electrons near the Fermi level are excited by the laser light. The energy thermalizes *via* electron–electron scattering, leading to an effective electron temperature on a femtosecond timescale. In a second step further thermalization occurs by electron–lattice scattering into phonon modes on a picosecond timescale. Desorption is induced by coupling to the hot electron bath or to the phonons. One recent example is the desorption of CO from Ru(001).<sup>2</sup>

In the case of infrared (IR) laser-induced processes, different degrees of freedom in the system are excited and different relaxation and desorption pathways exist, thus different scenarios apply. For molecules adsorbed on a surface three fundamental excitation and desorption scenarios can occur:

(1) The IR laser light excites the surface directly. This process leads to heating of the surface and to induced thermal desorption.

(2) The external bond between the molecule and the surface is resonantly excited by the IR radiation. When the excitation exceeds the binding energy, the molecule may desorb. This (multi-)photon excitation to the desorption continuum is only possible when the exciting laser light is able to overcome the anharmonicity of the external potential.

(3) The IR light excites resonantly an internal vibrational mode of the adsorbed molecule. This vibrational energy then has to couple to the desorption coordinate either directly or indirectly *via* energy transfer to the surface.

The dynamics of the desorption process will depend on the coupling and the energy flow between the different degrees of freedom.

The excitation and desorption process of molecules from surfaces after IR excitation has, for example, been investigated by Heidberg and coworkers<sup>3–8</sup> as well as by Chuang and coworkers.<sup>9–13</sup> In Heidberg's studies, a CO<sub>2</sub> laser emitting light at fixed frequencies was used as IR light source and the emission lines or their second harmonics were in accidental resonance with the adsorbates.<sup>3–8</sup> The internal stretching vibration of CO or the C–F stretching mode in CH<sub>3</sub>F adsorbed on NaCl(film)/NaCl(100) were excited. For both molecules, the desorption process occurs only when the excitation laser is resonant with a vibrational mode of the molecule. However, experiments on isotopically mixed layers of <sup>12</sup>CO and <sup>13</sup>CO as well as CH<sub>3</sub>F and CD<sub>3</sub>F showed no isotope selective desorption. These observations are indicating that the desorption involves either a resonant heating process or a  $\nu$ – $\nu$ -transfer followed by energy transfer from the excited internal vibration to the normal translational motion of the adsorbed molecule.<sup>6–8</sup>

Chuang *et al.* investigated the desorption of ammonia and pyridine from Cu(100) as well as from KCl- and Ag-films.<sup>9–13</sup> Either a CO<sub>2</sub>-laser or an IR source tunable in the frequency range between 2.5 and 4.2 μm was used to resonantly excite the internal stretching modes of the molecules. Based on isotopic mixture experiments, a thermal desorption mechanism *via* excitation of the internal mode is considered to be most likely in these experiments.

Desorption induced by IR excitation also attracted significant theoretical interest where different approaches to describe the process are used (see *e.g.* 14–16). Gortel *et al.* have employed a master equation perturbation approach, in a quantum-mechanical framework, which takes into account the rates of competing processes (like laser pumping, phonon-assisted (inelastic) and elastic decay of a resonance state, and thermalization of the surface bond) to determine the photodesorption rate.<sup>14</sup> Muckerman and Uzer have performed classical and

quantum-mechanical simulations for the intramolecular vibrational resonant photodesorption employing the Langevin model to describe the interaction of the adsorbed molecule with the heat bath.<sup>15</sup> Brivio *et al.* have used a classical Hamiltonian method to calculate the IR resonant photodesorption rates by applying a suitable average of classical trajectories calculated integrating the Hamilton's equations of motion.<sup>16</sup>

To study the excitation and desorption process, it is desirable to perform the experiments with a widely tunable IR source in order to be able to access different vibrational modes of the adsorbate. We have recently shown the feasibility of this by demonstrating the resonant infrared laser-induced desorption of N<sub>2</sub>O on NaCl(100) using the continuously tunable IR output of a free-electron laser.<sup>17</sup> Here, we will concentrate on the system CD<sub>3</sub>F condensed on NaCl(100) and discuss the desorption spectrum of the system, time-of-flight spectra, as well as the fluence dependence of the desorption signal.

## Experimental

The experiments reported here are performed in an ultrahigh vacuum (UHV) apparatus using the Free electron laser for infrared experiments (FELIX) user facility at our institute as a tunable infrared source.<sup>18</sup>

The UHV apparatus is a standard stainless steel chamber operating at a base pressure better than  $3 \times 10^{-10}$  mbar. The single crystal NaCl(100) samples are prepared by cleavage under dry nitrogen atmosphere and are transferred immediately into the vacuum. They are mounted to a copper sample holder for measurements in transmission geometry and fixed to it using molybdenum clamps. The sample temperature is monitored using NiCr–Ni and AuFe–Cr thermocouple pairs. The sample holder is connected to a cryostat that allows positioning of the sample in *x,y,z*-direction, a polar rotation by 360° and an azimuthal tilt. The sample can be cooled down to temperatures as low as 25 K using liquid helium. Between the measurements the surface is annealed to temperatures above 450 K. The laser light passes through the sample and exits the UHV chamber which is equipped with KBr windows. The angle of incidence onto the sample is 45° relative to the surface normal. The polarization of the infrared light is vertical. Detection of the desorbing neutral species is performed normal to the surface plane using electron impact ionization for ion detection in a differentially pumped quadrupole mass spectrometer (Extrel Q50). The distance between the surface and the electron impact ionization regime is 16 cm. The mass selected signal is recorded as a function of time after the laser pulse. Gas is admitted *via* background dosing using a leak valve. The gas inlet is made of stainless steel and operates at a base pressure below  $1 \times 10^{-6}$  mbar; no further purification of the CD<sub>3</sub>F gas (Matheson, >99 atom% D) was carried out.

Typically, a few hundred monolayers (ML) of CD<sub>3</sub>F are condensed under non-equilibrium conditions on the NaCl(100) single crystal surface at low temperature (30–40 K), using gas pressures in the range of  $1 \times 10^{-6}$  mbar. The coverage is estimated assuming a sticking coefficient of one. As an independent check in some experiments, the coverage is determined by linear absorption measurements using a FT-IR spectrometer (Bruker IFS66v). The adsorption temperature is chosen low enough to ensure that, on the time scale of the experiment, no significant thermal desorption occurs.

The IR output of FELIX is continuously tunable between 4.5 μm and 250 μm, although for the present desorption measurements only the wavelength range between 8 μm to 12 μm is used. FELIX produces pulsed IR radiation in so-called macropulses that consist of a series of micropulses. The micropulse duration varies, depending on the settings, between a few hundred femtoseconds and several picoseconds. The bandwidth is Fourier transform limited. The laser can be operated with

micropulse repetition rates of 25 MHz or 1 GHz, corresponding to a spacing of the micropulses of 40 and 1 ns, respectively. Macropulse energies can reach up to 100 mJ. For the present experiment, typical pulse energies are 0.5 mJ (25 MHz) and 15 mJ (1 GHz) per 6 to 7 μs long macropulse. The macropulse repetition rate is 5 Hz. The size of the laser spot on the surface is varied using a KBr lens (*f* = 470 mm). In all experiments reported here, the bandwidth of the IR beam is chosen to be below 0.5% of the central frequency, corresponding to a micropulse duration of a few picoseconds. Values reported for the laser energy are measured using a power meter directly in front of the KBr entrance window of the UHV chamber. The laser fluence is varied by using fixed value attenuators.

## Results

When the IR laser irradiates a multilayer of CD<sub>3</sub>F condensed on NaCl(100), at certain wavelengths and power settings, desorption of CD<sub>3</sub>F molecules is observed. The desorbing molecules are mass selectively detected using a differentially pumped quadrupole mass spectrometer. The fragmentation pattern in the mass-spectrum of the laser-induced desorbed CD<sub>3</sub>F is found to be identical to the one of the regular gas-phase CD<sub>3</sub>F, indicating that intact molecules are desorbed from the surface. Fig. 1a shows the desorption signal from a 500 ML thick CD<sub>3</sub>F film on NaCl(100) as a function of the IR wavelength in the spectral range from 850 to 1200 cm<sup>-1</sup>. Clearly, four separated peaks are observed located at 907, 958, 1066 and 1105 cm<sup>-1</sup>. The desorption spectrum can be compared to the linear absorption spectrum of a condensed CD<sub>3</sub>F film which is shown in Fig. 1b. A clear correspondence between those two spectra is found—all peaks that are

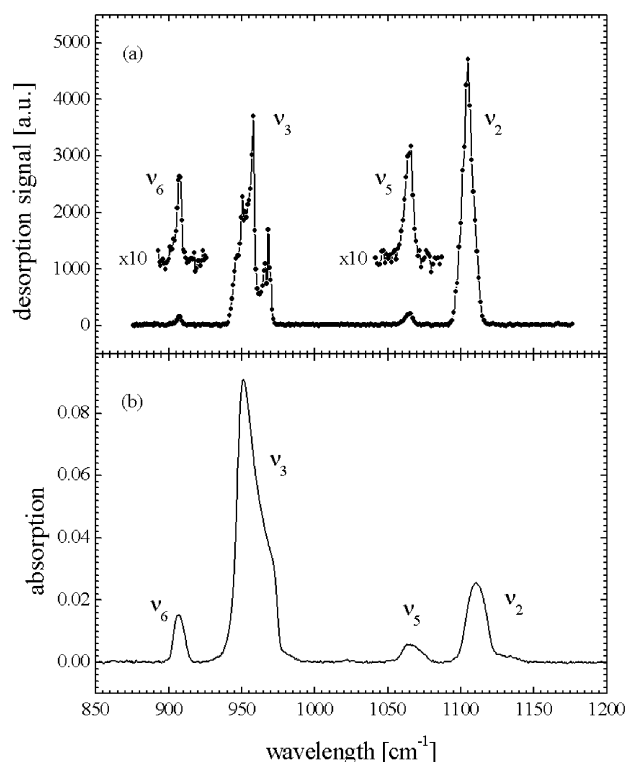


**Fig. 1** Desorption spectrum (a) and linear absorption spectrum (b) of CD<sub>3</sub>F condensed on NaCl(100). The film thickness is about 500 ML and the condensation temperature 40 K. Desorption is induced by FELIX operating at 25 MHz with a repetition rate of 5 Hz and focussed onto the surface. The desorption spectrum is recorded with a step-size of 0.01 μm, the linear IR spectrum with a resolution of 0.5 cm<sup>-1</sup>.

observed in the IR desorption spectrum have their counterparts in the linear absorption spectrum. According to convention, the peaks in the absorption spectrum are labeled  $\nu_2$ ,  $\nu_3$ ,  $\nu_5$ , and  $\nu_6$ .<sup>19</sup>

The peak positions in the desorption spectrum are, to within the spectral resolution of the IR light of FELIX, the same as in the absorption spectrum. The width of the desorption peaks that correspond to the  $\nu_5$  and  $\nu_6$  vibration is about  $8\text{ cm}^{-1}$ , comparable to the bandwidth of the IR laser. The  $\nu_2$  and especially the  $\nu_3$  mode are found to be significantly broader than this bandwidth. The  $\nu_3$  mode is observed to be split in the desorption spectrum and to consist of at least two components. This is consistent with the broad and asymmetric line in the linear absorption spectrum. A splitting of the non-degenerate  $\nu_2$  and  $\nu_3$  modes in  $\text{CD}_3\text{F}$  was already reported before.<sup>20</sup> Due to the lack of crystallographic data the underlying splitting mechanism can not be clarified unambiguously.

A comparison of relative intensities in the desorption and absorption spectra is difficult, since the signal in the desorption process may well depend non-linearly on IR power and fluence. Nevertheless, for the given experimental parameters it is evident that the intensities are different from those in the linear absorption spectrum. This holds especially true for the  $\nu_5$  and  $\nu_6$  modes which are observed to have significantly lower intensities in the desorption spectrum as compared to the linear absorption case.

To obtain the spectrum in Fig. 1a, the ion signal observed after the macropulse is integrated over time. There obviously is important information contained in the time-dependence of this ion signal. A selection of representative time-of-flight (TOF) spectra for  $\text{CD}_3\text{F}$  desorbing from  $\text{NaCl}(100)$  is shown in Fig. 2. They are recorded from a film of about 500 ML thickness at a condensation temperature of 40 K for three different laser fluences  $-32.6\text{ J cm}^{-2}$  (top),  $15.5\text{ J cm}^{-2}$  (middle) and  $9.3\text{ J cm}^{-2}$  (bottom). The left traces show the TOF spectra corresponding to the first laser pulse on a fresh surface spot. The center and the right traces give the spectra for the second and the tenth pulse onto the same spot. The TOF distributions from the following shots differ markedly from those of the first shots. The TOF spectrum of the first laser pulse is character-

ized by a higher intensity and the maximum flight time is considerably shorter, corresponding to faster molecules, than for the following pulses. There seems to be an abrupt change between the first and the second pulse, the differences between the following pulses are found to be much smaller. The intensity of the signal and the velocity of the desorbed molecules decrease in a more continuous way toward lower values. By comparing the TOF spectra recorded for the different laser fluences it is found that for the first laser pulse the most probable flight time shows a pronounced dependence on the laser fluence. The higher the fluence the higher is the kinetic energy of the molecules. For the next pulses this behavior is not observed anymore. There, the flight time seems to be more or less independent of the fluence, although the intensity is increasing with increasing laser fluence. The shape of the TOF distribution is determined by: (i) the time during which the neutrals are desorbed from the surface; (ii) their velocity distribution; (iii) the extent of the electron impact ionization region relative to the total flight distance from the surface to the electron impact ionization source; (iv) the dependence of the ionization efficiency on the particle velocity; and (v) the time it takes for an ionized species to reach the detector. The (short) flight time of the ions from the ionizer to the detector can be subtracted from the TOF distribution. In the case of an electron impact ionizer with a relatively low ionization efficiency (on the order of  $10^{-3}$ ), the ionization probability for a molecule is proportional to its residence time in the ionizer, thus inversely proportional to its velocity.

When the time during which desorption occurs is short compared to the width of the signal, the TOF distribution directly reflects the velocity distribution of the desorbed molecules and therefore contains information on the translational temperature of the desorbing species.

Under the prerequisite that the molecules leave the surface under thermal equilibrium conditions, a Maxwell-Boltzmann type of distribution is expected.<sup>21</sup>

$$f(t) = \frac{a}{t^{i+1}} \exp\left(-\frac{m}{2kT} \left(\frac{d}{t} - u\right)^2\right)$$

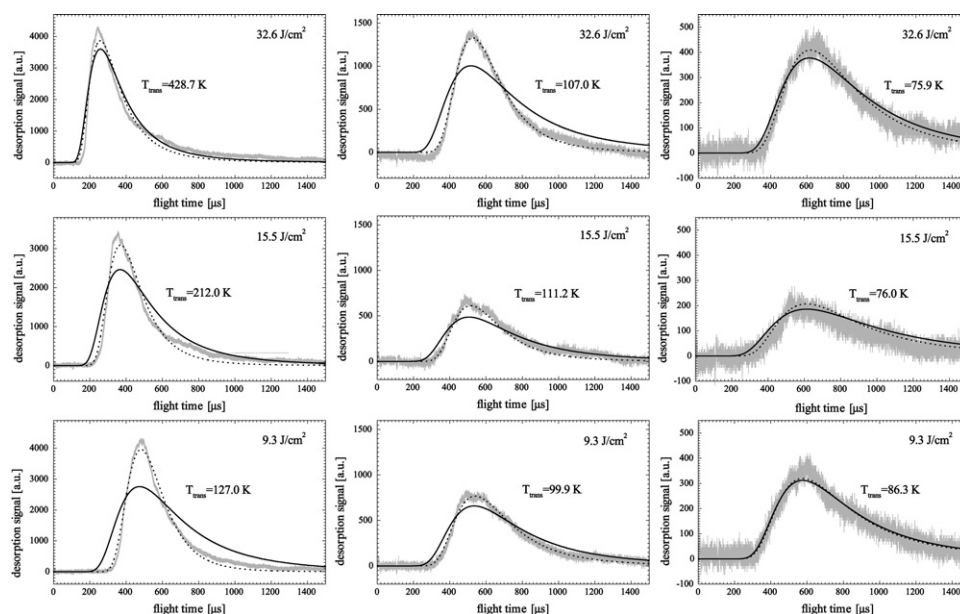


**Fig. 2** TOF spectra recorded for the desorption of  $\text{CD}_3\text{F}$  condensed on  $\text{NaCl}(100)$  ( $\sim 500\text{ ML}$  and  $T = 40\text{ K}$ ) at a IR wavelength of  $958\text{ cm}^{-1}$  for three different laser fluences  $I$  ( $32.6$ ,  $15.5$  and  $9.3\text{ J cm}^{-2}$ ). Desorption is induced by laser operation at  $1\text{ GHz}$  with a repetition rate of  $5\text{ Hz}$ . The left traces show the TOF spectra recorded for the first laser pulse irradiating the surface, the centre traces represent the second pulse and the right ones the tenth pulse onto the same surface spot. The grey line gives the experimental data, the full and the dashed lines represent the fitted spectrum employing the modified Maxwell-Boltzmann distribution without (full) and with (dashed) stream velocity. The translational temperatures given in the figure are derived from the fit without stream velocity.

Here  $a$  is a normalization constant,  $t$  is the flight time and  $d$  is the flight distance between sample and ionizer. The velocity is connected to the flight distance and flight time by  $v = d/t$ . The constant  $i$  equals 2 or 3 in case of a density (“ $v^2$ ”) or a flux weighted (“ $v^3$ ”) Maxwell distribution, respectively. In our experimental geometry, the ionization efficiency is inversely proportional to the velocity and  $i$  is thus 3. The quantity  $u$  is a constant to offset for a stream velocity due to collisions of the desorbing molecules in the gas phase.

The results of the best fits using the so-called modified Maxwell–Boltzmann distribution ( $i = 3$ ) without and with stream velocity  $u$  are given in Fig. 2 as full (without) and dashed (with) lines. In general, it turns out that with a stream velocity, substantially better fits can be obtained, showing that the TOF spectra are not determined by a purely thermal distribution. Due to the additional stream velocity, the resulting “temperature” in this case, however, is not well defined and therefore the determined translational temperatures are not considered for further data evaluation. The fits without stream velocity describe the main features of the measured TOF distributions—the rising and descending branch as well as the maximum of the flight time distribution. The fitted distributions appear to be slightly too broad compared to the measured distributions, especially for the first laser pulse as well as for the highest laser fluence. The translational temperatures of the desorbing  $\text{CD}_3\text{F}$  molecules determined from these fits range between 428.7 K and 75.9 K, all being well above the measured surface temperature of about 40 K. Fig. 3 summarizes the observed maxima of the flight time distribution as well as the determined translational temperatures as a function of the laser fluence for the first, second and tenth laser pulse onto the same surface spot.

## Discussion

The resonant character of the IR laser-induced desorption process is clearly demonstrated for  $\text{CD}_3\text{F}$  condensed on  $\text{NaCl}(100)$  by the desorption spectrum presented in Fig. 1a. In the whole series of measurements, under widely varying experimental conditions, non-resonant desorption signals have never been observed even for very high laser intensities. In addition, the temperature increase  $\Delta T$  of the  $\text{NaCl}$  substrate by direct laser-substrate coupling has been estimated as  $\Delta T \ll 1$  K.<sup>5</sup> Therefore, desorption induced by a direct surface heating process discussed as scenario (1) in the introduction

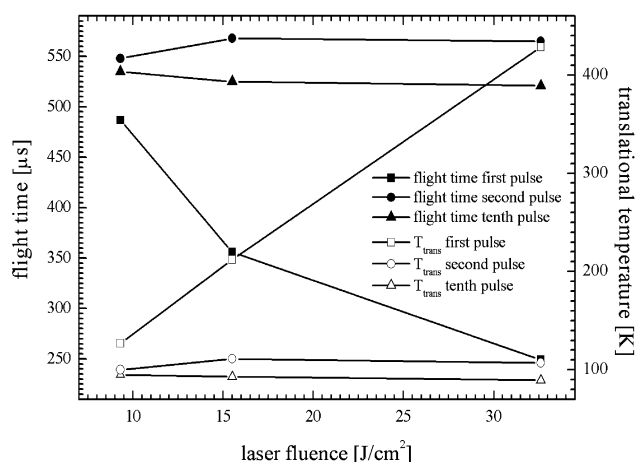


**Fig. 3** The maximum of the flight time distribution (solid symbols), determined from the TOF spectra of Fig. 2, and the translational temperatures (open symbols), derived from the fits using the modified Maxwell–Boltzmann distribution, are shown as a function of the laser fluence for the first (square), second (circle) and tenth (triangle) laser pulse irradiating the same surface spot.

can be excluded. It is evident that the initial step is the resonant excitation of the internal mode of the molecule, *i.e.* mechanism (3) described in the introduction. Following this excitation of an internal mode of the adsorbed molecule, several channels are open for energy dissipation and relaxation. At least two competitive channels are left as reasons for the observed desorption.

(a) Due to coupling of the excited molecules to the heat bath of the adsorbate layer, a temperature increase of the complete layer results. Desorption is induced if the temperature rise due to heating of the layer is sufficient to overcome the binding energy between the molecules. This process is accounted for as resonant heating. Due to the energy equilibration involved, the desorption is not limited to those molecules initially excited but can also involve neighboring or, in the case of mixed layers, also different molecules.

(b) When the vibrational energy that is stored in a molecule exceeds the binding energy between the molecules, direct desorption by elastic or inelastic “tunneling” into the desorption continuum becomes energetically feasible. For multi-photon processes stepwise multi-photon excitation or vibrational energy transfer between neighboring adsorbate molecules by resonant or quasi-resonant  $v$ - $v$ -transfer can be important. In both processes the anharmonicity compensation is assisted by low-frequency external modes and/or adsorbent phonons. If the process is fast enough, population of highly excited vibrational levels can occur. For  $\text{CO}$  adsorbed on  $\text{NaCl}(100)$  energy pooling up to  $v = 30$  has been observed.<sup>22</sup> In contrast to the resonant heating case this process keeps its molecule and isotope selectivity as only the molecules that are initially excited can then desorb.

In order to distinguish between these two desorption mechanisms, an analysis of the dependence of the desorption signal and the recorded TOF spectra on the IR power and fluence is useful. It is controversially discussed in the literature whether and under which conditions velocity distributions of desorbing molecules can be described using a thermal equilibrium model, *i.e.* fit by a Maxwellian type of distribution, and if those distributions deliver realistic values for the temperatures of the desorbing species.<sup>23–26</sup> One of the prerequisites for application is local thermal equilibrium – the energy is locally statistically distributed over all degrees of freedom. In the present investigation, an internal mode of a molecule condensed on a single crystal surface is initially excited. It is a priori not clear, on what time-scale this energy relaxes. To our knowledge only one experimental study on the lifetimes of excited vibrational states of molecules adsorbed or condensed on insulator single crystal surfaces is reported. The system under study –  $\text{CO}/\text{NaCl}(100)$  – was resonantly vibrationally excited using a cw  $\text{CO}$  laser. From the observed spectrally resolved fluorescence the lifetime of the  $\text{CO}$  stretching vibration is found to be in the range of a few milliseconds,<sup>22,27,28</sup> which would not meet the requirements. Such long lifetimes, however, seem to be incompatible with the observed desorption signal in our experiment that corresponds to prompt after the IR pulse.

As can be seen in Figs. 2 and 3, when fitting a modified Maxwell–Boltzmann distribution to the experimental TOF distributions, a good fit of the TOF spectra is obtained and translational temperatures higher than the substrate temperature are derived. In addition, a non-linear dependence of the translational temperature on the applied laser fluence is found. The higher the laser fluence the faster the molecules become and furthermore, the molecules desorbing with the first laser pulse have a higher translational temperature than the ones desorbed with the following pulses.

Such a behavior is in general in agreement with a resonant heating mechanism [case (a)], where under the assumption of thermal equilibrium higher translational temperatures are expected for larger energy absorption. For higher laser intensities

ties the layer is heated faster and to higher temperatures. This means that the desorbing molecule carries more kinetic energy when leaving the surface corresponding to a shorter flight time. As a function of the irradiation time the layer thickness decreases and a laser pulse can only deposit less energy in the adsorbate. A coupling to the heat bath leads then to a lower maximal temperature and a longer flight time results.

For the alternative direct desorption mechanism [case (b)], the translational temperature will, in principle, be determined by the amount of excess energy remaining in the molecule after desorption and the degree of freedom carrying this energy. To a first approximation, these quantities are expected to be almost independent of the laser intensity and pretreatment of the surface by the laser (assuming no structural changes are induced). In the experiments it is observed that the translational temperature depends strongly on the laser fluence as well as on the adsorbate conditions, which makes the direct desorption process less likely.

On the other hand, it is found that the experimental distribution is in most cases narrower than the fitted distribution. This is rather surprising, since any delayed desorption process or a possible temperature gradient on the surface would lead to distributions that are broader than a thermal distribution. Further, it is found that the experimental distributions become narrower, when the amount of desorbed molecules is high. From this, one might be tempted to conclude that direct desorption does play a role. However, these observations can also be rationalized by the occurrence of collisions of desorbing molecules in the gas phase. Those collisions can lead to adiabatic cooling similar as in a supersonic expansion used in molecular beams. This adiabatic cooling will result in a narrower velocity distribution with an increased average velocity. If post-desorption collisions in the gas-phase are important, the actual temperature of the molecules while desorbing is significantly lower than the temperatures indicated in the figure. Further measurements concerning the dependence of the desorption process on the layer thickness and the laser fluence can address this issue and will be undertaken.

Presently, we are working on a numerical model to get more insight into the question of the underlying desorption mechanism for the laser-induced desorption of small molecules from insulator surfaces. Results will be presented in a forthcoming publication.

## Conclusions

Resonant IR laser-induced desorption of multilayers of CD<sub>3</sub>F condensed on NaCl(100) single crystal surfaces using tunable infrared light is reported. After resonant excitation of intramolecular vibrations of CD<sub>3</sub>F, desorption is observed. In the desorption spectrum four infrared active fundamental modes are unambiguously identified. The spectral features of the desorption spectrum are comparable to the linear absorption spectrum of condensed CD<sub>3</sub>F. TOF spectra are investigated as a function of the laser energy and as a function of the number of laser pulses irradiating a sample spot and yield translational temperatures well above the original surface temperature. The observed dependencies on laser energy and

layer thickness are compatible with a resonant heating process as desorption mechanism.

## Acknowledgements

The authors gratefully acknowledge the FELIX staff for technical support. This work was supported by the FOM and the Deutsche Forschungsgemeinschaft (Za 110/11). B. R. thanks the Deutsche Forschungsgemeinschaft for a fellowship in the Emmy-Noether-Programm.

## References

- 1 *Laser Spectroscopy and Photochemistry on Metal Surfaces*, ed. H.-L. Dai and W. Ho, *Advanced Series in Physical Chemistry*, vol. 5, World Scientific, Singapore, 1995.
- 2 (a) M. Bonn, S. Funk, Ch. Hess, D. N. Denzler, C. Stampfl, M. Scheffler, M. Wolf and G. Ertl, *Science*, 1999, **285**, 1042; (b) M. Bonn, C. Hess, S. Funk, J. H. Miners, B. N. J. Persson, M. Wolf and G. Ertl, *Phys. Rev. Lett.*, 2000, **84**, 4653; (c) S. Funk, M. Bonn, D. N. Denzler, Ch. Hess, M. Wolf and G. Ertl, *J. Chem. Phys.*, 2000, **112**, 9888.
- 3 J. Heidberg, H. Stein, E. Riehl and A. Nestmann, *Z. Phys. Chem. (Munich)*, 1980, **121**, 145.
- 4 J. Heidberg, H. Stein and E. Riehl, *Phys. Rev. Lett.*, 1982, **49**, 666.
- 5 J. Heidberg, H. Stein, E. Riehl, Z. Szilagy and H. Weiss, *Surf. Sci.*, 1985, **158**, 553.
- 6 J. Heidberg, U. Noseck, M. Suhren and H. Weiss, *Ber. Bunsen-Ges. Phys. Chem.*, 1993, **97**, 329.
- 7 J. Heidberg, H. Stein and H. Weiss, *Surf. Sci.*, 1987, **184**, L431.
- 8 J. Heidberg, K.-W. Stahmer, H. Stein and H. Weiss, *J. Electron Spectrosc. Relat. Phenom.*, 1987, **45**, 87.
- 9 T. J. Chuang, *Surf. Sci. Rep.*, 1983, **3**, 1.
- 10 T. J. Chuang and H. Seki, *Phys. Rev. Lett.*, 1982, **49**, 382.
- 11 T. J. Chuang, H. Seki and I. Hussla, *Surf. Sci.*, 1985, **158**, 525.
- 12 T. J. Chuang and I. Hussla, *Phys. Rev. Lett.*, 1984, **52**, 2045.
- 13 T. J. Chuang, *Surf. Sci.*, 1986, **178**, 783.
- 14 (a) Z. W. Gortel, H. J. Kreuzer, P. Piercy and R. Teshima, *Phys. Rev. B*, 1983, **27**, 5066; (b) Z. W. Gortel, H. J. Kreuzer, P. Piercy and R. Teshima, *Phys. Rev. B*, 1983, **28**, 2119.
- 15 J. T. Muckerman and T. Uzer, *J. Chem. Phys.*, 1989, **90**, 1968.
- 16 (a) G. P. Brivio and Z. W. Gortel, *Surf. Sci.*, 1992, **261**, 359; (b) G. P. Brivio and M. Torri, *Phys. Rev. B*, 1993, **48**, 4835.
- 17 B. Redlich, H. Zacharias, G. Meijer and G. von Helden, *Surf. Sci.*, 2002, **502/503**, 325.
- 18 D. Oepts, A. F. G. van der Meer and P. W. van Amersfoort, *Infrared Phys. Technol.*, 1995, **36**, 297.
- 19 G. Herzberg, *Molecular Spectra and Molecular Structure. II. Infrared and Raman Spectra of Polyatomic Molecules*, Krieger Publishing Company, Malabar, Florida, 1991.
- 20 T. J. Chao and D. F. Eggers, *J. Chem. Phys.*, 1977, **66**, 970.
- 21 F. M. Zimmermann and W. Ho, *Surf. Sci. Rep.*, 1995, **22**, 127.
- 22 H.-C. Chang and G. E. Ewing, *J. Phys. Chem.*, 1990, **94**, 7635.
- 23 Z. W. Gortel, H. J. Kreuzer, M. Schäff and G. Wedler, *Surf. Sci.*, 1983, **134**, 577.
- 24 K. Witan, D. Borgmann and G. Wedler, *Appl. Phys. A*, 1990, **51**, 132.
- 25 B. Schäfer and P. Hess, *Appl. Phys. B*, 1985, **37**, 197.
- 26 M. Buck and P. Hess, *J. Electron Spectrosc. Relat. Phenom.*, 1987, **45**, 237.
- 27 H.-C. Chang, C. Noda and G. E. Ewing, *J. Vac. Sci. Technol. A*, 1990, **A8**, 2644.
- 28 H.-C. Chang and G. E. Ewing, *Phys. Rev. Lett.*, 1990, **65**, 2125.